Gel formation through reversible and irreversible aggregation

2009 J. Phys.: Condens. Matter 21 504109

(http://iopscience.iop.org/0953-8984/21/50/504109)

IOP PUBLISHING JOURNAL OF PHYSICS: CONDENSED MATTER

J. Phys.: Condens. Matter **21** (2009) 504109 (7pp) doi:10.1088/0953-8984/21/50/504109

Gel formation through reversible and irreversible aggregation

Piero Tartaglia

Dipartimento di Fisica and CNR-INFM-SMC, Università di Roma La Sapienza,
Piazzale Aldo Moro 2, I-00185, Roma, Italy

Received 8 May 2009, in final form 11 May 2009
Published 23 November 2009
Online at stacks.iop.org/JPhysCM/21/504109

Abstract

We study the kinetics of formation of branched loopless structures in mixtures of particles with different shapes and functionalities. These systems are treated with the appropriate Smoluchowski rate equations, including condensation and fragmentation terms, and it is shown that it is possible to provide a parameter-free description of the assembly process, including the limit of irreversible aggregation at low temperatures. Using dynamics simulations we provide evidence of a connection between physical and chemical gelation in low-valence particle systems, and the possibility of relating ageing time with temperature.

1. Introduction

Self-assembly through aggregation is a ubiquitous process that can be observed in various situations of technological and biomedical interest at a number of length and timescales. Examples are polymer chemistry, aerosol systems, cloud physics, clusters of galaxies in astrophysics, etc and as a consequence the physics behind the formation of branched structures and networks, starting from monomeric unassembled initial states, is receiving considerable attention in both molecular and supramolecular systems [1–7].

Aggregation in colloidal suspensions has been studied in recent years in great detail since it gives rise to both non-equilibrium and equilibrium phenomena. The final stage of the aggregation may lead to the formation of an extended three-dimensional network of bonds connecting independent molecules, proteins or colloidal particles, the resulting material being a gel. At the gel point, a persistent network spanning the sample first appears, the system is then prevented from flowing yet is not arrested on a mesoscopic length scale. A distinction is made between irreversible and reversible aggregation, based on the values of the ratio of the attraction energy to the thermal energy $u_0/(k_BT)$. The final percolating structure formed by these processes is called a chemical or a physical gel, due to irreversible or reversible clustering, respectively. When u_0 is much larger than k_BT the particles tend to form bonds that are not destroyed by thermal agitation, and as a consequence progressively form larger and larger clusters, ending in a structure spanning the entire sample [8], a process called chemical gelation. The aggregate often results in fractal structures, whose dimension is controlled by the kinetics of the process [9]. During irreversible aggregation, bonds never break and the final structure of the aggregates results from a delicate balance between the cluster size dependence of the diffusion process and the probability to irreversibly stick. Chemical gelation has been extensively studied in the past, starting from the pioneering work of Flory [10] and Stockmayer [11] who developed the first mean field description of gelation, providing expressions for the cluster size distribution as a function of the extent of reaction or bond probability $p(t)$, the ratio of the number of bonded links to the total number of links, and the critical behavior of the connectivity properties close to gelation. Flory and Stockmayer (FS) derived the basic relations between $p(t)$ and the resulting structure in step polymerizations, under the assumptions that all functional groups of a given type are equally reactive, all groups react independently of one another, and that ring formation does not occur in molecular species of finite size. Only when p exceeds a critical value p_c can infinitely large molecules grow [10]. In this respect the FS theory describes the gelation transition as the random percolation of permanent bonds on a loopless lattice [12]. In reversible aggregation, bond-breaking events are possible since $u_0 \lesssim k_BT$ and the equilibrium state, which can also percolate, is characterized by a distribution of clusters which continuously restructure on a timescale controlled by the bond lifetime. The value of the ratio u_0/k_BT separates the two classes, but any model of physical aggregation may be turned into a chemical model by studying its properties following a quench to $k_BT \ll u_0$. Analogously, applying temperatures comparable to the bond energy turns an irreversible aggregation model into a physical one.

The idea of a close connection between irreversible and reversible aggregation is already contained in the early mean field theoretical work of Stockmayer, who solved the Smoluchowski kinetic equations in the limit of absence of closed bonding loops. In Stockmayer calculations, at any time during chemical aggregation, the distribution of clusters of finite size is identical to that found following equilibrium statistical mechanics by maximizing the entropy with the constraint of a fixed number of bonds. Later on, Van Dongen and Ernst [13] confirmed that the FS distributions are also solutions of the Smoluchowski equations when bond-breaking processes are accounted for. According to these theoretical works a system forming progressively larger loopless branched aggregates evolves in time via a sequence of states, identical to the states explored in equilibrium for appropriate values of the temperature. The equality in the fraction of formed bonds provides the connection between time during reversible or irreversible aggregation and temperature in equilibrium. Van Dongen and Ernst also provided an analytical expression for the time dependence of the bond probability following a sudden change in the external control parameters, offering the first soluble example of reversible self-assembly of loopless branched structures.

In this paper we will review the Smoluchowski mean field theory for reversible and irreversible aggregation, along the lines of approach of van Dongen and Ernst for a binary system of particles, where the number of reactive sites on the monomers, called functionality, is 2 and f. We will then describe a set of molecular dynamics simulations for reversible and irreversible clustering in order to verify the predictions and the limits of the theory.

2. Solution of the Smoluchowski equation

The starting point of the theoretical approach is the Smoluchowski equation for coagulation, where, in order to allow for reversible aggregation leading to a steady state, a step in which the aggregates break up in smaller units is inserted in the rate equations. We consider a binary system made of N monomers of functionality f and L monomers of functionality 2, the case relevant for the simulations we performed. We denote by $c_{i,l}$ a cluster containing i monomers of functionality f and l monomers of functionality 2 and by $N_{i,l}$ the number of such clusters, also $c_{i,l} = N_{i,l}/(N + L)$.

The processes taken into account describe growth of aggregates through

(i) formation of large clusters $c_{i,l}$ from coalescence of two smaller clusters;
(ii) disappearance of clusters $c_{i,l}$ due to formation of larger aggregates.

and are represented by the reactions

$$\begin{aligned} c_{j,m} + c_{i-j,l-m} &\underset{F_{j,i-j,m,l-m}}{\overset{K_{j,i-j}}{\rightleftarrows}} c_{i,l}, \\ c_{i,l} + c_{j,m} &\underset{F_{i,j,l,m}}{\overset{K_{i,j}}{\rightleftarrows}} c_{i+j,l+m}, \end{aligned} \tag{1}$$

with reaction rates given by $K_{i,j}$, while the inverse reactions of cluster break-up are characterized by the rates $F_{i,j,l,m}$. The asymmetry of the rates will be made clear in what follows. As both coagulation and fragmentation are allowed, the coagulation equations become

$$\frac{\mathrm{d}c_{i,l}(t)}{\mathrm{d}t} = \frac{1}{2}\sum_{j+j'=i}\sum_{m+m'=l}(c_{j,m}K_{j,j'}c_{j',m'} - F_{j,j',m,m'}c_{j+j',m+m'}) - \tag{2}$$

$$\sum_{j=0}^{\infty}\sum_{m=0}^{\infty}(c_{i,l}K_{i,j}c_{j,m} - F_{i,l,j,m}c_{i+j,l+m}), \tag{3}$$

and are usually complemented with the initial conditions, e.g. only monomers present $c_{i,l}(0) = (N\delta_{i,1}\delta_{l,0} + L\delta_{i,0}\delta_{l,1})/(N + L)$. The coalescence and fragmentation of clusters are dominated essentially by two effects, due to the mobility and the bonding phases of the aggregation. The first one is related to the diffusive motion of the clusters in the system, the second to the mechanism of the bonding reaction between clusters. Correspondingly it is possible to distinguish the following two limiting cases which depend on the diffusion and aggregation timescales [14]:

(i) Aggregation is limited by the reaction mechanism, when diffusion is fast and bonding slow, so that the rate-controlling step is the chemical reaction leading to clustering.
(ii) Aggregation is limited by slow diffusion and high sticking probabilities of the aggregates, the chemical limit of the aggregation process.

The overall rate constants include both the properties of the transport of clusters and the bonding reactions and are determined by the physical system under investigation. In particular we consider two different types of aggregation, corresponding respectively to the specific reaction mechanism at the basis of bonding, $K^{\mathrm{b}}_{i,j}$, and the time spent by the clusters in diffusing between coalescence events, $K^{\mathrm{d}}_{i,j}$. The total reaction rate can be written as

$$\frac{1}{K_{i,j}} = \frac{1}{K^{\mathrm{b}}_{i,j}} + \frac{1}{K^{\mathrm{d}}_{i,j}}. \tag{4}$$

In the case of aggregation based on diffusion, $K^{\mathrm{d}}_{i,j} \ll K^{\mathrm{b}}_{i,j}$ and the leading reaction dominates so that the limiting step is diffusion, and $K_{i,j} \approx K^{\mathrm{d}}_{i,j}$ while for the case in which the coagulation kinetics dominates $K^{\mathrm{b}}_{i,j} \ll K^{\mathrm{d}}_{i,j}$ since diffusion is efficient, then $K_{i,j} \approx K^{\mathrm{b}}_{i,j}$. In other words the clustering process is controlled by the slowest step but depends on the microscopic dynamics and on the range of the site–site interaction. Indeed, only when the site–site interaction is short-ranged is the probability that two sites on distinct clusters interact, in the absence of any activation barrier, particularly small. As a consequence the time required to form a bond between two nearby clusters can be significantly longer than the time required for two clusters of any size to diffuse over distances comparable to the inter-cluster distances.

Reaction dominated kernels are represented by the well known RA_f model for polycondensation or polymerization,

i.e. bonding of monomers in the case in which they possess two, three or more adhesive points on their surface. The RA_f model was studied by FS using the bond formation probability as a parameter, without reference to the kinetic rate equations, and subsequently shown to be a solution to the Smoluchowski equations at any time. Regarding the absence of bond loops in the aggregates, we stress that both the fact that a small fraction of particle orientations allows the particles to bond and the fact that the average functionality is very small are important elements favoring the formation of loopless aggregates [7]. Specificity in the bond interaction and limited valence are thus crucial for the validity of the above assumptions, according to which $K_{i,j}$ is proportional to the number of distinct ways in which a cluster of size i can bond a cluster of size j, and $F_{i,j,l,m}$ is proportional to the number of distinct ways in which a cluster can break into two clusters of size i and j for $f \neq 2$ and l and m for $f = 2$, the coefficients of proportionality K_S and F_S being, respectively, the rate constants of forming and breaking a single bond [13]. Since the monomers consist of f-functional reactive endgroups when two monomers react, the resulting dimer has $2f - 2$ reactive endgroups, a trimer has $3f - 4$ endgroups, and a general i-mer has $if - 2(i - 1)$ endgroups, or $\sigma_i = (f - 2)\, i + 2$ free bonds, when loops are not allowed. In the RA_f model, since all end groups are equally reactive, the reaction rate between two clusters equals the product of the number of end groups, thus $K_{i,j} = K_S\, \sigma_i\, \sigma_j$.

Following Stockmayer, the total number of ways to distribute the $N+L$ particles to form the distribution of clusters $N_{i,l}$ is given by

$$\Omega = N!L! \prod_{i=1}^{N} \prod_{l=1}^{L} {w_{i,l}}^{N_{i,l}} \frac{1}{N_{i,l}!}, \tag{5}$$

where $i!l!w_{i,l}$ is the number of ways in which i and l monomers, with functionalities f and 2, respectively, form a cluster $c_{n,l}$

$$w_{i,l} = f^i 2^l \frac{(fi - i + l)!}{i!l!\sigma_i!}, \tag{6}$$

with $\sigma_i = (f - 2)i + 2$. The recursion relation

$$(i + l - 1)w_{i,l} = \tfrac{1}{2} \sum_{j=0}^{i-1} \sum_{m=0}^{l-1} \sigma_j \sigma_{i-j} w_{j,m} w_{i-j,l-m}, \tag{7}$$

is also needed to derive the solution. The most probable distribution is obtained by maximizing with respect to $N_{i,l}$ under the constraint of constant total numbers of monomers N, L and total number of clusters N_c,

$$N = \sum_{i=0}^{N} \sum_{l=0}^{L} i N_{i,l} \qquad L = \sum_{i=0}^{N} \sum_{l=0}^{L} l N_{i,l}$$
$$N_c = \sum_{i=0}^{N} \sum_{l=0}^{L} N_{i,l}. \tag{8}$$

The values $N_{i,l}$ that minimize Ω are more transparently written in terms of the parameter p, which is the ratio of the number of bonded links to the total number of links $p = 2(N + L - N_c)/(fN + 2L)$ as

$$c_{i,l} = A w_{i,l} \xi^i \eta^l, \tag{9}$$

with the Lagrange multipliers

$$A = \bar{f} \frac{(1-p)^2}{p}, \qquad \xi = \frac{N}{(N+L)} \frac{p(1-p)^{f-2}}{\bar{f}},$$
$$\eta = \frac{L}{(N+L)} \frac{p}{\bar{f}}, \tag{10}$$

which yields

$$c_{i,l} = \bar{f} \frac{(1-p)^2}{p} \left[\frac{N}{(N+L)} \frac{p(1-p)^{f-2}}{\bar{f}} \right]^i \times \left[\frac{L}{(N+L)} \frac{p}{\bar{f}} \right]^l w_{i,l}, \tag{11}$$

with the average functionality defined by $\bar{f} = (fN + 2L)/(N + L)$.

We then impose the conditions of detailed balance at equilibrium needed to get a steady state solution

$$K_{j,j'} c_{j,m}(\infty) c_{j',m'}(\infty) = F_{j,j',m,m'} c_{j+j',m+m'}(\infty), \tag{12}$$

expressing the fact the number of clusters created by aggregation must be equal to the number of clusters disappearing by fragmentation. This equation gives an expression for the segmentation rate

$$F_{j,j',m,m'} = A(\infty) K_{j,j'} \frac{w_{j,m} w_{j',m'}}{w_{j+j',m+m'}} = F_S \sigma_j \sigma_{j'} \frac{w_{j,m} w_{j',m'}}{w_{j+j',m+m'}}, \tag{13}$$

where $F_S = A(\infty) K_S$ is the rate for single bond fragmentation. Using (9) in the Smoluchowski equation we obtain

$$\frac{\mathrm{d}c_{i,l}(t)}{\mathrm{d}t} = \left[1 - \frac{A(\infty)}{A(t)} \right] \times \left[\tfrac{1}{2} \sum_{j+j'=i} \sum_{m+m'=l} c_{j,m} K_{j,j'} c_{j',m'} - \sum_{j=0}^{\infty} \sum_{m=0}^{\infty} c_{i,l} K_{i,j} c_{j,m} \right] \tag{14}$$

and the rate equations have the usual form for irreversible aggregation, provided that the time is changed $t \to \tau$ according to the rule

$$\mathrm{d}\tau = \left[1 - \frac{A(\infty)}{A(t)} \right] \mathrm{d}t, \tag{15}$$

and the evolution equation for $p(t)$ is given by

$$\frac{1}{K_S} \frac{\mathrm{d}p}{\mathrm{d}t} = \bar{f}\, (1-p)^2 - A(\infty) p. \tag{16}$$

The solution of this equation, with initial condition $p_0 = \lim_{t \to 0} p(t)$, is

$$p(t) = p_\infty \frac{1 - \Lambda \mathrm{e}^{-\Gamma t}}{1 - p_\infty^2\, \Lambda \mathrm{e}^{-\Gamma t}}, \tag{17}$$

where $p_\infty = \lim_{t \to \infty} p(t)$ and

$$p_\infty = 1 + \frac{A(\infty)}{2\bar{f}} - \sqrt{\frac{A(\infty)}{\bar{f}} \left[1 + \frac{A(\infty)}{4\bar{f}} \right]}, \tag{18}$$

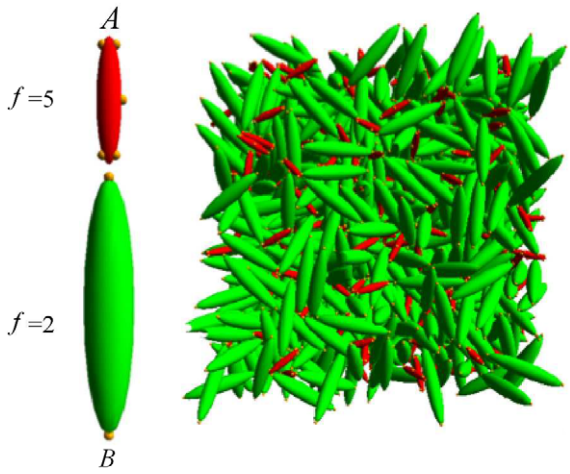

Figure 1. Graphic description of the A and B type particles (left) and snapshot of the simulated system (right). The centers of the small spheres locate the bonding sites on the surface of the hardcore particle.

(This figure is in colour only in the electronic version)

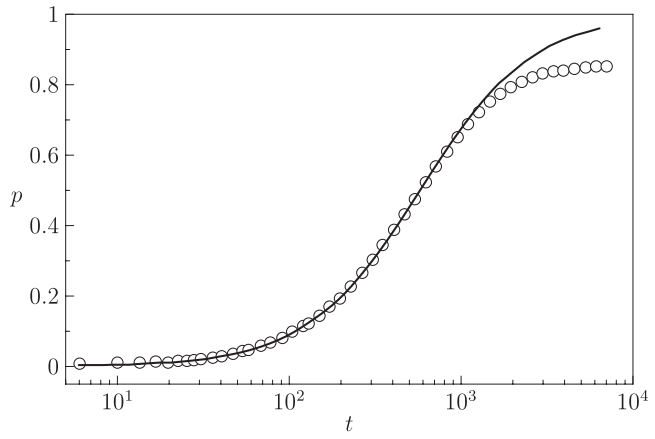

Figure 2. Time dependence of the fraction of bonds $p(t)$ during irreversible aggregation. Symbols are the simulation results while the solid line is the solution of the Smoluchowski kinetic equation.

$$\Gamma = 2K_S\,\bar{f}\sqrt{\frac{A(\infty)}{\bar{f}}\left[1+\frac{A(\infty)}{4\bar{f}}\right]} = K_S\bar{f}\frac{1-p_\infty^2}{p_\infty}, \quad (19)$$

$$\Lambda = \frac{1}{1-p_0p_\infty}\left(1-\frac{p_0}{p_\infty}\right). \quad (20)$$

In the limit $A(\infty) \to 0$ one recovers the irreversible aggregation solution. The important point to note here is that the FS solution is valid at each instant provided that the bond probability is the appropriate function of time.

In the post-gelation regime, when a percolating cluster is present, we assume the Flory hypothesis according to which all reactive groups located on an isolated cluster or on the gel remain equally reactive.

In the following sections we will discuss the comparison of the theory with the results obtained using molecular dynamics simulations of various systems, subject to irreversible or reversible clustering.

3. Irreversible aggregation of ellipsoidal patchy particles

To study the dynamics of the irreversible gelation process and the evolution of the cluster size distribution a model inspired by the formation of epoxy resin [15] from pentafunctional diethylenetriamine (A particles) and bifunctional diglycidyl-ether of bisphenol-A (B particles) was used. To incorporate excluded volume and shape effects both molecules are represented as hard homogeneous ellipsoids of appropriate length, whose surface is decorated in a predefined geometry by f identical reactive sites per particle (see figure 1). The evolution of the system is studied via event-driven molecular dynamics simulations, where the particles evolve through Newtonian dynamics and bind irreversibly every time the distance between two unreacted sites, on particles of opposite type, becomes smaller than a predefined distance δ. The system consists of a 5:2 binary mixture composed of $N_A = 480$ ellipsoids of type A and $N_B = 1200$ ellipsoids of type B, for a total of $N = 1680$ particles. Type A particles are modeled as hard ellipsoids of revolution with axes $a = b = 2\sigma$ and $c = 10\sigma$ and mass m; type B particles have axes $a = b = 4\sigma$ and $c = 20\sigma$, mass 3.4 m. Simulations are performed at temperature $T = 1.0$ and packing fraction $\phi = 0.3$. Note that temperature only controls the timescale of exploration of space by modulating the average particle's velocity. In the initial configuration there are only monomers. During the evolution, every time two reactive sites get closer than $delta = 0.2\sigma$, a bond is formed. To model irreversible gelation, once a bond is formed it is made irreversible by switching on an infinite energy barrier at distance $r_{AB}^{ij} = \delta$ between the sites involved (i, j) which prevents the formation of new bonds in the same sites and the breaking of the existing one. The model satisfies the conditions of equal and independent reactivity of all reactive sites. Moreover, even if the absence of closed bonding loops is not explicitly implemented the condition is realized. In fact it is favored by the small flexibility of the bonded particles and their non-spherical shape.

The fraction $p(t)$ of bonds formed, which measures the extent of the reaction, increases monotonically until most of the particles are connected in one single cluster and saturates around 0.86, as shown in figure 2. The time dependence of $p(t)$ is found to agree with the theoretical predictions for loopless aggregation, with percolation expected at $p_c = 0.5$ that is located at $p_c = 0.505 \pm 0.007$.

4. Reversible aggregation of ellipsoidal patchy particles

The previous model of loopless clusters was extended to the physical gel case by including a finite attraction strength between bonding sites, which offers the possibility of carefully checking the theoretical predictions. In particular we could test the prediction that reversible aggregation dynamics is represented by a sequence of equilibrium states, with the result of closely connecting time and temperature.

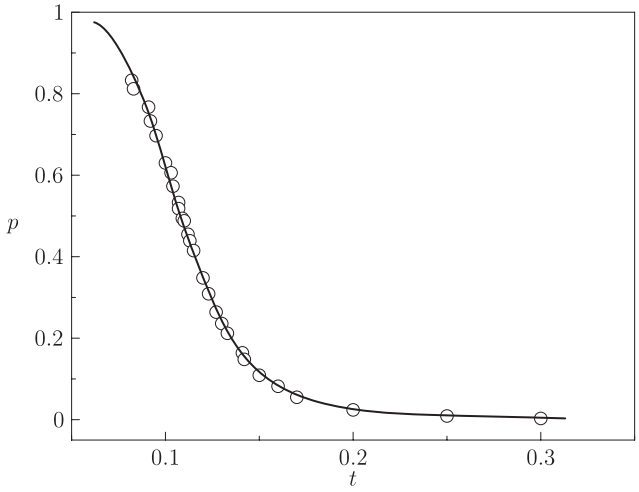

Figure 3. Temperature dependence of p_∞, with $p_c = 0.5$ the percolation threshold. Symbols are simulation results while the solid line represents (21) with $\Delta S/k_B = 8.52$ the best fitted value.

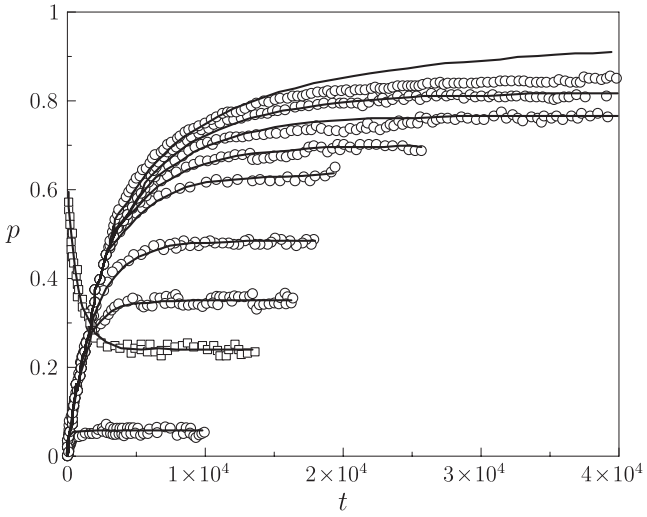

Figure 4. Time dependence of the fraction of bonds during reversible aggregation at different temperatures ($T = 0.17, 0.13, 0.12, 0.11, 0.10, 0.095, 0.09, 0.082, 0.07$) from the lower to the higher equilibrium value, starting from an unbonded configuration ($p_0 = 0$; circles) or from a generic equilibrated configuration ($p_0 \neq 0$; squares). Lines are solutions of the Smoluchowski equation for reversible aggregation.

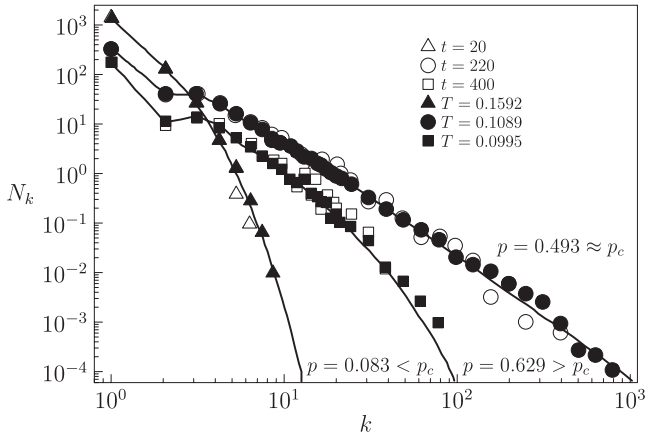

Figure 5. Cluster size distribution N_k. Equilibrium results (closed symbols) are compared with results at different times during irreversible aggregation (open symbols) using the correspondence $p(t) = p_\infty(T)$. The solid lines are FS predictions.

We studied [16] via event-driven molecular dynamics simulations a binary mixture composed of $N_A = 480$ pentafunctional ($f_A = 5$) ellipsoids of type A and $N_B = 1200$ bifunctional ($f_B = 2$) ellipsoids of type B, so that the number of A-type reactive sites equals the number of B-type reactive sites. The shapes and masses of the particles are the same as used in the case of irreversible aggregation. The interaction potential is the hard ellipsoid potential supplemented by site–site square-well attractive interactions (of strength u_0, and width $\delta = 0.2\sigma$) between pairs of particles of different type. The unit mass is m, the unit energy u_0. Temperature is measured in units of the potential depth (i.e. $k_B = 1$) and time in units of $\sigma(m/u_0)^{1/2}$. The volume fraction is fixed at $\phi = 0.3$ and T is varied from $T = 0.3$ to 0.065. Two sites, on particles of different types, form a bond if their distance is closer than δ and each site is engaged in one bond at most. Starting from a set of monomers, during the simulation at fixed temperature bonds form and break continuously, while the system evolves toward the equilibrium state, characterized by the equilibrium value $p_\infty(T)$.

Figure 3 shows the equilibrium $p_\infty(T)$ for many temperature values and the rather accurate theoretical representation given by the independent-bond mass-action law [17]

$$\frac{p_\infty}{(1-p_\infty)^2} = e^{\beta(u_0 - T\Delta S)} \tag{21}$$

where u_0 and ΔS are the energy and the entropy change associated with the formation of a single bond. Figure 4 shows the time dependence of the bond probability in a temperature jump experiment, starting either from a high temperature monomer configuration where $p(0) = 0$ or from an equilibrated configuration characterized by branched aggregates $p(0) \neq 0$. Lines in figure 3 are the theoretical predictions with the Flory post-gel assumption [10] for $p(t) > p_c$. The theoretical expression represents the numerical data very well, except for $T \leqslant 0.07$ when extensively bonded states are reached, probably due to a failure of the Flory assumption above the gel point.

Figure 5 shows the cluster size distribution N_k for three different values of T, corresponding to p_∞ values below, at and above $p_c = 0.505 \pm 0.007$. Since, following the FS approach, we expect that during irreversible aggregation the system will follow a series of equilibrium states, we establish a correspondence with reversible aggregation states at constant temperature according to the rule $p(t) = p_\infty(T)$. At each instant, data are identical to those obtained in equilibrium at the same bond probability, demonstrating that the evolution of the system structure and connectivity during irreversible aggregation does follow a sequence of equilibrium states.

To summarize, a system of ellipsoidal shaped particles with a limited set of attractive spots on their surface does

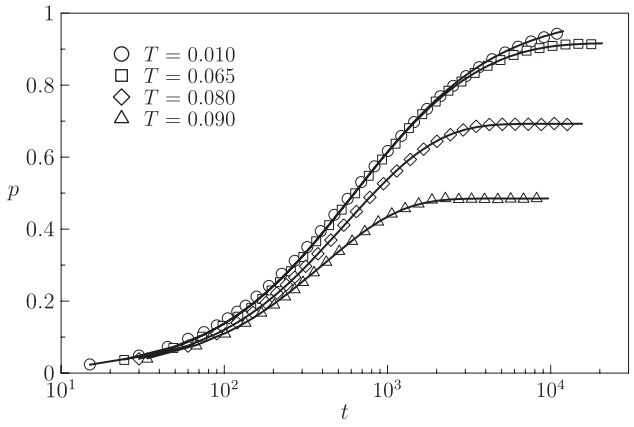

Figure 6. Evolution of the bond probability for $\rho = 0.0382$ at three different temperatures, $T = 0.09$, 0.08 and 0.065, and for an irreversible aggregation case $T = 0.01$. Lines are solutions of the Smoluchowski equations.

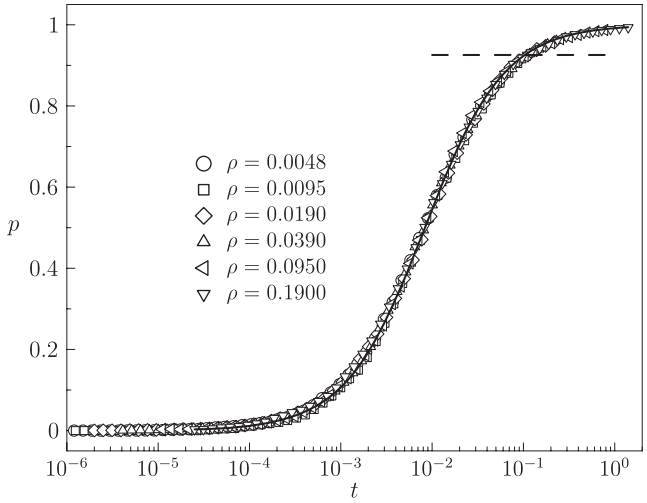

Figure 7. Evolution of the bond probability $p(t)$ in an irreversible aggregation process, quenched to $T = 0.01$, for several different starting densities ρ as a function of the variable $\bar{f}\rho\Delta_{\mathrm{W}}t$. The dashed line indicates the percolation threshold $p = 0.9256$.

not generate loops of inter-particle bonds, and forms cluster by aggregation dominated by bonding and not by diffusion, and is well described by a mean field approach. In particular the kinetics can be fully described, without fitting parameters, by combining a thermodynamic approach of the Wertheim type with the Smoluchowski kinetic equations including coagulation and fragmentation terms. This applies to both reversible and irreversible aggregation of branched systems.

5. Reversible aggregation of low functionality spherical patchy particles

We also performed [18] Brownian dynamics simulations of a binary mixture of 2835 particles with functionality $f = 2$ and 165 particles with $f = 3$, i.e. average functionality $\bar{f} = 2.055$, at several values of density and temperature, a model whose equilibrium properties have been well characterized recently [7]. Particles are hard spheres of diameter $\sigma = 1$ with a surface decorated by two or three interacting sites. Sites on different particles interact via a square-well potential of depth $u_0 = 1$ and interaction range $\delta = 0.119\sigma$. The high-T limit of this model is the hard-sphere fluid. On cooling, particles bond to each other, forming polydisperse clusters which then percolate and assemble, on further cooling, into a network of long-lived bonds. The phase diagram of the system includes a percolation line defined by the value $p_\infty = 0.9256$ [7]. We studied the evolution of the system at constant ρ, after a T-jump starting from a high-T unbonded configuration. Temperature is measured in units of u_0, while time is measured in reduced units such that $t = 1$ corresponds to the time required to diffuse a distance equal to the particle diameter.

The equilibrium condition for the bond probability derived from (16) is

$$\frac{p_\infty}{(1-p_\infty)^2} = \bar{f}\frac{K_{\mathrm{S}}}{K_{\mathrm{F}}} \tag{22}$$

and allows a connection with the thermodynamic perturbation theory of Wertheim for associated liquids [7] which gives an expression for the same quantity as a function of density and temperature

$$\frac{p_\infty}{(1-p_\infty)^2} = \rho f \Delta_{\mathrm{W}}(\rho)(\mathrm{e}^{\beta u_0} - 1), \tag{23}$$

thus permitting a connection with the kinetic approach of Smoluchowski. $\Delta_{\mathrm{W}}(\rho)$ can be calculated analytically, and in terms of σ and δ one finds, indicating with $\phi = \frac{\pi}{6}\sigma^3\rho$ the volume fraction,

$$\Delta_{\mathrm{W}} = \frac{\pi\delta^4(15\sigma + 4\delta)/30\sigma^2}{(1-\phi)^3} \times \left[1 - \frac{5}{2}\frac{(3\sigma^2 + 8\delta\sigma + 3\delta^2)}{\sigma(15\sigma + 4\delta)}\phi - \frac{3}{2}\frac{(12\delta\sigma + 5\delta^2)}{\sigma(15\sigma + 4\delta)}\phi^2\right]. \tag{24}$$

One can then predict the T and ρ dependence of the ratio between the single bond reaction rates and, apart from a constant related to the timescale and the chosen particle dynamics, provide a parameter-free description of the evolution of the entire aggregation process.

Figure 6 shows the time dependence of p following the T quench at constant density, starting from monomers and approaching equilibrium. Figure 7 shows the time evolution of $p(t)$ following a quench to a very low temperature, $T = 0.01$, equivalent to irreversible kinetics. Data at different densities collapse on a master curve when reported as a function of $\bar{f}\rho\Delta_{\mathrm{W}}t$, as predicted by the irreversible limit of (17) and the Wertheim relation (23).

In this case too the structure of the system during equilibration follows a sequence of equilibrium states as predicted by the theory, as shown in figure 8. It gives the cluster size distribution N_k of the system in equilibrium at four distinct values of T and fixed ρ, and the corresponding quantities during the equilibration process evaluated at times t_w chosen according to the relation $p(t_w) = p_\infty(T)$. We stress once again that mapping equilibrium and ageing properties

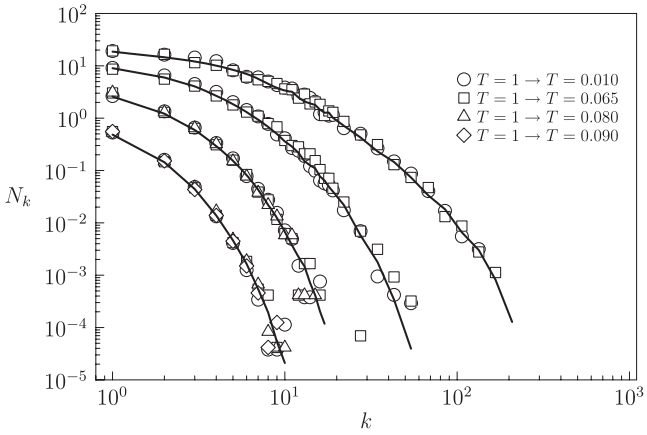

Figure 8. Comparison between equilibrium (full lines) and ageing (symbols) structural properties for $\rho = 0.0038$. The equilibrium data refer to $T = 0.1, 0.09, 0.08$ and 0.07 at $\rho = (6/\pi)0.02$. The ageing data refer to different equilibration processes, always starting from the high temperature $T = 1$ where the system is composed only of monomers, to several different final temperatures indicated in the labels. Data refer to different times following the quench, t_w, chosen in such a way that $p(t_w) = p_\infty(T)$.

hold only in the limit of loopless aggregating clusters, which in turn implies small functionality. In fact it can be shown [19] that systems with average functionality $\bar{f} \lesssim 2.8$ have a negligible number of loops and fulfill rather well the mean field predictions. Moreover diffusion does not play a relevant role in the rate constants; these are mainly influenced by the difficulty in interacting with the right orientation to form a bond, due in turn to the range of attraction between sites which must be small.

Acknowledgments

Support from NoE SoftComp NMP3-CT-2004-502235 is acknowledged. This paper reports work done in collaboration with S Corezzi, C De Michele, D Fioretto, E La Nave, J Russo, F Sciortino and E Zaccarelli in the last 2 years.

References

[1] Lehn J M 2002 *Proc. Natl Acad. Sci.* **99** 4763
[2] de Greef T F A and Meijer E W 2008 *Nature* **453** 171
[3] Cordier P, Tournilhac F, Soulie-Ziakovic C and Leibler L 2008 *Nature* **451** 977
[4] Manoharan V N, Elsesser M T and Pine D J 2003 *Science* **301** 483
[5] Mirkin C, Letsinger R, Mucic R and Storhoff J 1996 *Nature* **382** 607
[6] Zaccarelli E 2007 *J. Phys.: Condens. Matter* **19** 323101
[7] Bianchi E, Tartaglia P, La Nave E and Sciortino F 2007 *J. Phys. Chem.* B **111** 11765
[8] Martin J and Adolf D 1991 *Annu. Rev. Phys. Chem.* **42** 311
[9] Vicsek T 1989 *Fractal Growth Phenomena* (Singapore: World Scientific)
[10] Flory P J 1953 *Principles of Polymer Chemistry* (London: Cornell University Press)
[11] Stockmayer W H 1943 *J. Chem. Phys.* **11** 45
[12] Stauffer D and Aharony A 1992 *Introduction to Percolation Theory* (London: Taylor and Francis)
[13] van Dongen P G J and Ernst M H 1984 *J. Stat. Phys.* **37** 301
[14] Oshanin G and Moreau M 1995 *J. Chem. Phys.* **102** 2977
[15] Corezzi S, De Michele C, Zaccarelli E, Fioretto D and Sciortino F 2008 *Soft Matter* **4** 1173
[16] Corezzi S, De Michele C, Zaccarelli E, Tartaglia P and Sciortino F 2009 *J. Phys. Chem.* B **113** 1233
[17] Wertheim M J 1984 *J. Stat. Phys.* **35** 19
[18] Sciortino F, De Michele C, Corezzi S, Russo J, Zaccarelli E and Tartaglia P 2009 *Soft Matter* at press
[19] Russo J, Tartaglia P and Sciortino F 2009 *J. Chem. Phys.* submitted